

Non-Commutativity of the Zero Chemical Potential Limit and the Thermodynamic Limit in Finite Density Systems

J. Ambjørn*

*The Niels Bohr Institute, Blegdamsvej 17, 2100 Copenhagen, Denmark and
Institute for Theoretical Physics, Utrecht University,
Leuvenlaan 4, 3584 CE Utrecht, The Netherlands*

K.N. Anagnostopoulos†

*Department of Physics, University of Crete, P.O. Box 2208, GR-71003 Heraklion, Greece and
Physics Department, National Technical University, Zografou Campus, GR-15780 Athens, Greece*

J. Nishimura‡

High Energy Accelerator Research Organization (KEK), 1-1 Oho, Tsukuba 306-0801, Japan

J.J.M. Verbaarschot§

Department of Physics and Astronomy, SUNY, Stony Brook, NY 11794, USA

(Dated: July 18, 2018)

Monte Carlo simulations of finite density systems are often plagued by the complex action problem. We point out that there exists certain non-commutativity in the zero chemical potential limit and the thermodynamic limit when one tries to study such systems by reweighting techniques. This is demonstrated by explicit calculations in a Random Matrix Theory, which is thought to be a simple qualitative model for finite density QCD. The factorization method allows us to understand how the non-commutativity, which appears at the intermediate steps, cancels in the end results for physical observables.

PACS numbers: 05.10.Ln, 11.25.-w, 11.25.Sq

I. INTRODUCTION

QCD at finite baryon density and/or finite temperature has attracted much attention due to its relevance to the physics of the early universe, heavy ion collisions and neutron stars. It is of particular importance to explore the phase diagram in the μ (chemical potential), T (temperature) plane, where interesting phases such as a superconducting phase have been conjectured to appear. Monte Carlo simulations, which enable first-principle studies at $\mu = 0$, are hindered by the fact that the fermion determinant becomes complex for $\mu \neq 0$. The standard reweighting method uses the absolute value for generating configurations, and takes account of the phase in measuring observables. Due to cancellations caused by the oscillating phase, however, the required number of configurations grows exponentially with the system size. Furthermore the method suffers from the so-called overlap problem, which is caused by the mismatch of the region in the configuration space which contributes to the ensemble average and the region which one mostly samples in the phase-quenched model.

One of the recent developments in this direction is that

the reweighting techniques have proven to be of use in exploring the phase diagram at small μ and large T , where the fluctuation of the phase is still under control. Substantial improvements are achieved by various tricks such as the multi-parameter reweighting [1, 2], Taylor expansion approach [3] and the imaginary μ approach [4, 5]. In particular the first approach was able to locate the critical end point in the μ - T plane [2]. (See also Ref. [6].)

In Ref. [7] two of the authors (K.N.A. and J.N.) proposed a new method, the factorization method, for simulating systems with complex actions. The method utilizes the fact that the distribution of observables factorizes into the corresponding distribution for the phase-quenched model and the weight factor representing the effect of the phase. Each factor can be obtained by constrained Monte Carlo simulations, which eliminate the overlap problem completely. The knowledge of the weight factor allows us to understand the effect of the phase intuitively. The method is quite general, and in particular it is expected to be useful in going beyond the small μ regime in finite density QCD. The method proposed for simulating θ -vacuum like systems [8] may be viewed as a particular case of the factorization method. In Ref. [9] it was pointed out that the factorization method belongs to the class of methods known as ‘the density of states method’.

In Ref. [10] we have tested the method in a Random Matrix Theory (RMT), which is thought of as a schematic model for QCD at finite baryon density [11]. RMT was originally introduced to describe the spectrum

*Electronic address: ambjorn@nbi.dk

†Electronic address: konstant@physics.uoc.gr

‡Electronic address: jnishi@post.kek.jp

§Electronic address: verbaarschot@tonic.physics.sunysb.edu

of the Dirac operator and has been extensively studied in the literature [12]. The model we have studied exhibits a first order phase transition at some value of the “chemical potential” and can be solved analytically even for finite size matrices [13]. One hopes to capture the essential properties of real QCD, while at the same time having a testing ground [14] for methods to be applied to real QCD. Indeed the factorization method is quite successful in RMT [10], where exact results are reproduced with great accuracy, and one understands clearly how the phase of the determinant induces the first order phase transition.

In this paper we investigate this model further in order to address the question of the non-commutativity in the $\mu \rightarrow 0$ limit and the thermodynamic limit. The factorization method allows us to understand how the non-commutativity appears at the intermediate steps of reweighting techniques, and how it cancels in the end results for physical observables. Preliminary results have already been presented in conference proceedings, Refs. [15, 16].

II. RMT FOR FINITE DENSITY QCD AND THE MONTE CARLO METHODS

We consider the RMT defined by the partition function

$$Z = \int dW e^{-N \text{tr}(W^\dagger W)} \det D, \quad (\text{II.1})$$

where W is a $N \times N$ complex matrix, and D is a $2N \times 2N$ matrix given by

$$D = \begin{pmatrix} m & iW + \mu \\ iW^\dagger + \mu & m \end{pmatrix}. \quad (\text{II.2})$$

The above model can be thought of as a schematic model of finite density QCD with one flavor, where the parameters μ and m correspond to the chemical potential and the quark mass respectively. The size of the matrix W corresponds to the number of low lying modes of the Dirac operator and if the density of these modes is taken to be unity, N can be interpreted as the volume of space-time. As physical observables, one may consider the “chiral condensate” and the “quark number density” defined by

$$\Sigma = \frac{1}{2N} \text{tr}(D^{-1}), \quad (\text{II.3})$$

$$\nu = \frac{1}{2N} \text{tr}(\gamma_4 D^{-1}), \quad \gamma_4 = \begin{pmatrix} 0 & \mathbb{1} \\ \mathbb{1} & 0 \end{pmatrix}. \quad (\text{II.4})$$

In what follows we consider the massless case ($m = 0$) and focus on the “quark number density”.

The model was first solved in the large- N limit [11], but an analytic solution has been obtained in [13] even for finite N . The partition function can be expressed as

$$Z(\mu) = \pi e^\kappa N^{-(N+1)} N! \left[1 + \frac{(-1)^{N+1}}{N!} \gamma(N+1, \kappa) \right], \quad (\text{II.5})$$

where $\kappa = -N\mu^2$ and $\gamma(n, x)$ is the incomplete γ -function defined by

$$\gamma(n, x) = \int_0^x e^{-t} t^{n-1} dt. \quad (\text{II.6})$$

From this one obtains the vacuum expectation value (VEV) of the quark number density as

$$\langle \nu \rangle = \frac{1}{2N} \frac{\partial}{\partial \mu} \ln Z(\mu) \quad (\text{II.7})$$

$$= -\mu \left[1 + \frac{\kappa^N e^{-\kappa}}{(-1)^{N+1} N + \gamma(N+1, \kappa)} \right]. \quad (\text{II.8})$$

In Fig. 1 we plot $\langle \nu \rangle$ as a function of the chemical potential μ for $N = 8, 16, 32, 64, 128$. The large- N limit of this formula is easily found by applying the saddle-point method to the incomplete γ -function. We obtain

$$\lim_{N \rightarrow \infty} \langle \nu \rangle = \begin{cases} -\mu & \text{for } \mu < \mu_c \\ 1/\mu & \text{for } \mu > \mu_c \end{cases}, \quad (\text{II.9})$$

where μ_c is the solution to the equation $1 + \mu^2 + \ln(\mu^2) = 0$, and its numerical value is given by $\mu_c = 0.527 \dots$. We find that the quark number density $\langle \nu \rangle$ has a discontinuity at $\mu = \mu_c$. Thus the schematic model reproduces qualitatively the first order phase transition expected to occur in ‘real’ QCD at nonzero baryon density.

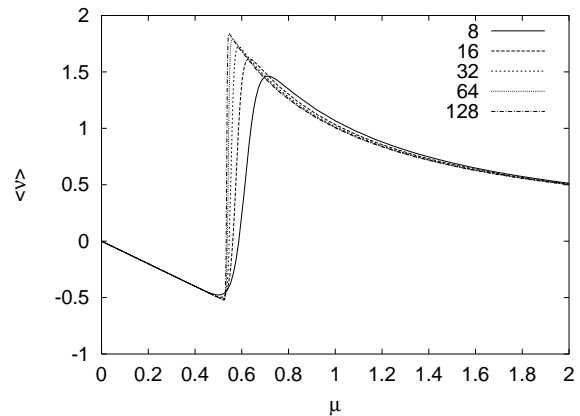


FIG. 1: The exact result (II.8) for the ‘quark number density’ $\langle \nu \rangle$ is plotted as a function of the ‘chemical potential’ μ for $N = 8, 16, 32, 64, 128$. In the $N \rightarrow \infty$ limit, the function develops a discontinuity at $\mu = \mu_c = 0.527 \dots$.

The model (II.1) cannot be simulated directly because the fermion determinant has a non-zero phase Γ defined by

$$\det D = e^{i\Gamma} |\det D|, \quad (\text{II.10})$$

when $\mu \neq 0$. In order to reveal the importance of the phase let us consider the *phase-quenched* model

$$Z_0 = \int dW e^{-N \text{tr}(W^\dagger W)} |\det D|$$

$$= \int dW e^{-S_0} , \quad (\text{II.11})$$

$$S_0 = N \text{tr}(W^\dagger W) - \ln |\det D| , \quad (\text{II.12})$$

and the corresponding VEVs, which we denote as $\langle \dots \rangle_0$. The large- N limit of $\langle \nu \rangle_0$ can be obtained analytically as [11]

$$\lim_{N \rightarrow \infty} \langle \nu \rangle_0 = \begin{cases} \mu & \text{for } \mu < 1 \\ 1/\mu & \text{for } \mu > 1 . \end{cases} \quad (\text{II.13})$$

Comparing this with the result (II.9) for the full model, we see that the effect of Γ is dramatic for $\mu < 1$.

The reweighting method uses the identity

$$\langle \nu \rangle = \frac{\langle \nu e^{i\Gamma} \rangle_0}{\langle e^{i\Gamma} \rangle_0} \quad (\text{II.14})$$

to calculate $\langle \nu \rangle$ for the full model by Monte Carlo simulation of the phase-quenched model. Due to the symmetry of the phase-quenched model under $W \mapsto -W$, where the fermion determinant $\det D$ as well as the observable ν becomes complex conjugate, we obtain

$$\langle \nu \rangle = \langle \nu_R \rangle + i \langle \nu_I \rangle , \quad (\text{II.15})$$

$$\langle \nu_R \rangle = \frac{\langle \nu_R \cos \Gamma \rangle_0}{\langle \cos \Gamma \rangle_0} , \quad (\text{II.16})$$

$$\langle \nu_I \rangle = i \frac{\langle \nu_I \sin \Gamma \rangle_0}{\langle \cos \Gamma \rangle_0} , \quad (\text{II.17})$$

where ν_R and ν_I denote the real part and the imaginary part of ν , respectively. The same symmetry implies that

$$\langle \nu_R \rangle_0 = \langle \nu \rangle_0 \quad ; \quad \langle \nu_I \rangle_0 = 0 . \quad (\text{II.18})$$

For the unquenched model, on the other hand, one obtains [10]

$$\langle \nu_R \rangle = 0 \quad ; \quad \langle \nu_I \rangle = i \mu \quad (\text{II.19})$$

in the large N limit for $\mu < \mu_c$, which is in sharp contrast to the phase-quenched result (II.18).

The factorization method in the present case amounts to calculating the VEVs on the r.h.s. of (II.16) and (II.17) by the formulae

$$\langle \nu_R \cos \Gamma \rangle_0 = \int_{-\infty}^{\infty} dx x \rho_R^{(0)}(x) w_R(x) , \quad (\text{II.20})$$

$$\langle \cos \Gamma \rangle_0 = \int_{-\infty}^{\infty} dx \rho_R^{(0)}(x) w_R(x) , \quad (\text{II.21})$$

$$\langle \nu_I \sin \Gamma \rangle_0 = 2 \int_0^{\infty} dx x \rho_I^{(0)}(x) w_I(x) , \quad (\text{II.22})$$

where the functions $\rho_i^{(0)}(x)$ ($i = R, I$) represent the distribution of ν_i ($i = R, I$) in the phase-quenched model

$$\rho_i^{(0)}(x) \stackrel{\text{def}}{=} \langle \delta(x - \nu_i) \rangle_0 . \quad (\text{II.23})$$

The weight factors $w_i(x)$ in Eqs. (II.20)–(II.22) are defined by

$$w_R(x) \stackrel{\text{def}}{=} \langle \cos \Gamma \rangle_{R,x} , \quad (\text{II.24})$$

$$w_I(x) \stackrel{\text{def}}{=} \langle \sin \Gamma \rangle_{I,x} , \quad (\text{II.25})$$

where the VEV $\langle \dots \rangle_{i,x}$ is taken with respect to yet another partition function

$$Z_i(x) = \int dW e^{-S_0} \delta(x - \nu_i) . \quad (\text{II.26})$$

The problem then reduces to the calculation of the four functions $\rho_i^{(0)}(x)$ and $w_i(x)$ ($i = R, I$). This may be done in various ways. In Ref. [10] as well as in the present work we have simulated

$$Z_{i,V} = \int dW e^{-S_0} e^{-V(\nu_i)} , \quad (\text{II.27})$$

where the δ -function in (II.26) is replaced by a sharply peaked potential $V(x)$, which is taken to be Gaussian

$$V(x) = \frac{1}{2} \gamma (x - \xi)^2 \quad (\text{II.28})$$

with γ and ξ being real parameters. By choosing γ large enough, the results become insensitive to its value (we used $\gamma = 1000.0$). The functions $\rho_i^{(0)}(x)$ can be obtained from the same simulation. We refer the reader to Ref. [10] for more details.

The complex action problem occurs in the reweighting method because the trigonometric functions in (II.16) and (II.17) flip their signs violently when one moves around the configuration space. The same problem occurs in the factorization method when one calculates the weight factors (II.24), (II.25). However, by simulating the constrained system (II.27), one forces the simulation to sample the important region of the configuration space, which is rarely visited by the simulation of the phase-quenched model (II.11). Thus the factorization method removes the overlap problem completely. Once the weight factors are obtained roughly, one can make the sampling more efficient by the use of multi-canonical simulations. This is not yet done, however. The knowledge of the weight factors is also useful in understanding the effect of the phase intuitively [7, 10], and it plays a crucial role in the present work.

III. NON-COMMUTATIVITY OF THE $\mu \rightarrow 0$ AND THE THERMODYNAMIC LIMIT

In this Section we discuss the non-commutativity of the two limits $\mu \rightarrow 0$ and $N \rightarrow \infty$ in the RMT. Such non-commutativity can be readily seen from the partition function (II.5). Below the critical point, the large N behavior is given by $Z(\mu) \sim \text{const.} e^{-N\mu^2}$. Omitting the μ -independent factor, the partition function approaches

unity if one takes the $\mu \rightarrow 0$ limit first, whereas it vanishes if one takes the large N limit first. More generally, one obtains e^{-C} , if one takes the two limits simultaneously with fixed $N\mu^2 \equiv C$. This non-commutativity is caused by the phase of the determinant. The phase vanishes at $\mu = 0$ for finite N , and one obtains a nonzero result for the partition function in the large N limit with appropriate normalization. If one takes the large N limit first for small but finite μ , however, the oscillation of the phase becomes violent, and as a result one obtains $Z = 0$ with the same normalization.

We note, however, that the free energy defined by

$$f(\mu) = - \lim_{N \rightarrow \infty} \left\{ \frac{1}{N} \ln Z(\mu, N) - \text{const.} \right\} \quad (\text{III.29})$$

after subtracting the μ -independent constant is given by $f(\mu) = \mu^2$ at $\mu < \mu_c$, which is continuous at $\mu = 0$ [20]. Furthermore we find from (II.8) or Fig. 1 that the quark number density does not have such non-commutativity, either. Thus the non-commutativity does not seem to appear in physical quantities, but it appears at the intermediate steps of the reweighting method as we will see in what follows.

Let us first consider the weight factor $w_R(x)$, which has a non-commutativity similar to the partition function. Since the phase Γ disappears identically for $\mu = 0$, one obtains $w_R(x) \equiv 1$ at $\mu = 0$ for any N . On the other hand, one obtains $w_R(x) \equiv 0$ in the large N limit for any $\mu \neq 0$, since the phase oscillates violently. In Fig. 2 we plot $w_R(x)$ for $\mu = 0.1$ and $\mu = 0.2$ at $N = 8, 16, 32$. The weight factor $w_R(x)$ crosses zero, and the crossing point moves to infinity as $\mu \rightarrow 0$. Thus the convergence of $w_R(x)$ to $w_R(x) \equiv 1$ in the $\mu \rightarrow 0$ limit is *not* uniform.

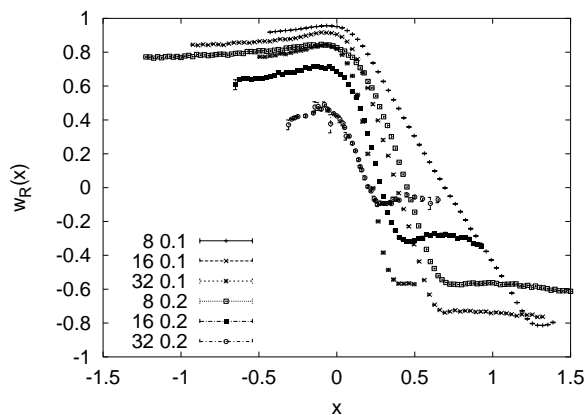


FIG. 2: The weight factor $w_R(x)$ is plotted for $\mu = 0.1$ and 0.2 at $N = 8, 16, 32$.

As μ approaches zero for fixed N , a linear regime develops in the region where $w_R(x)$ crosses zero. We extract the slope $\sigma_R(\mu, N)$ in this regime and plot it against μ in Fig. 3. At small μ we find that the slope can be fitted nicely by

$$\sigma_R(\mu, N) \sim -\alpha_R(N) \mu, \quad (\text{III.30})$$

where the coefficient $\alpha_R(N)$ grows linearly with N . Therefore the asymptotic behavior of the weight factor $w_R(x)$ depends on how the two limits $\mu \rightarrow 0$, $N \rightarrow \infty$ are taken.

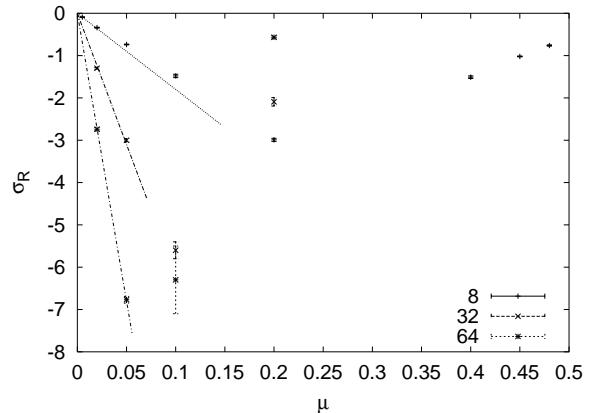


FIG. 3: The slope $\sigma_R(\mu, N)$ of the weight factor $w_R(x)$ in the linear regime is plotted against μ for $N = 8, 32, 64$. For sufficiently small μ it fits well to $\sigma_R(\mu, N) \sim -\alpha_R(N) \mu$.

Let us next turn to $\rho_R^{(0)}(x)$. In Fig. 4 we plot it for various N at $\mu = 0.2$. At small N the distribution is peaked near the origin and the dependence on N is small. As we go to larger N the peak moves to $x \sim 0.2$ and starts to grow. The VEV $\langle \nu_R \rangle_0$, which represents the position of the peak, is therefore close to zero at small N , and it approaches $\langle \nu_R \rangle_0 = \mu$ in the large N limit.

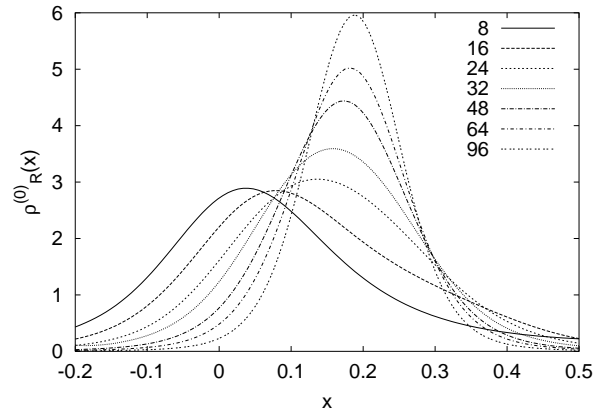


FIG. 4: The distribution $\rho_R^{(0)}(x)$ of ν_R in the phase-quenched model is plotted for $\mu = 0.2$ at various N .

In Fig. 5 we plot $\langle \nu_R \rangle_0 - \mu$ against $1/N$ for various μ . We see that the large N asymptotic behavior is given by

$$\langle \nu_R \rangle_0 = \mu - C(\mu) \frac{1}{N} + \dots, \quad (\text{III.31})$$

where the coefficient $C(\mu)$ grows as $\sim \frac{0.2}{\mu}$ for $\mu \rightarrow 0$.

From this one finds that the large N scaling sets in at

$$N \gg N_{\text{tr}} \simeq \frac{0.2}{\mu^2}. \quad (\text{III.32})$$

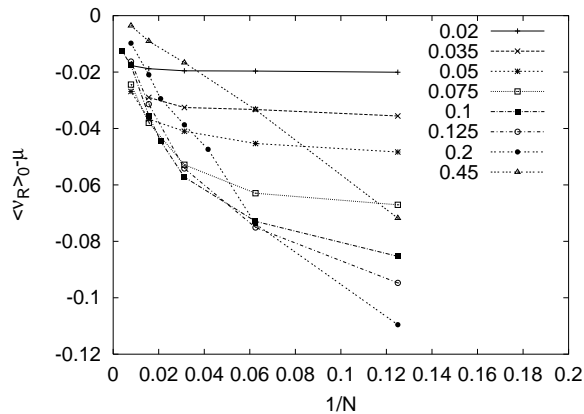


FIG. 5: We plot $\langle \nu_R \rangle_0 - \mu$ against $1/N$ for various μ .

The product $\rho_R^{(0)}(x) w_R(x)$ gives the unnormalized distribution of ν_R in the full model, which we plot in Fig. 6. The distribution itself, even after appropriate normalization, has the non-commutativity which is inherited from $\rho_R^{(0)}(x)$ and $w_R(x)$. However, the VEV $\langle \nu_R \rangle$, which is the first moment of the distribution, is always close to zero as one can see from Table I. The reason depends on whether $\mu \ll \frac{1}{\sqrt{N}}$ or $\mu \gg \frac{1}{\sqrt{N}}$. In the former case the distribution is peaked around the origin, which makes the first moment close to zero. In the latter case the positive and negative regions of the distribution cancel each other in the calculation of the first moment. Thus the non-commutativity cancels in the end result for the VEV $\langle \nu_R \rangle$. The situation for the imaginary part $\langle \nu_I \rangle$ is discussed in the Appendix.

N	$\langle \nu_R \rangle$	$i \langle \nu_I \rangle$	$\langle \nu \rangle$
8	0.0056(6)	-0.1970(5)	-0.1915(7)
16	0.0060(4)	-0.1905(13)	-0.1845(13)
24	0.0076(9)	-0.1972(14)	-0.1896(17)
32	0.0021(8)	-0.1947(19)	-0.1927(25)
48	0.0086(37)	-0.2086(54)	-0.2000(88)

TABLE I: The VEVs $\langle \nu_R \rangle$, $i \langle \nu_I \rangle$ and $\langle \nu \rangle$ obtained by the factorization method for $\mu = 0.2$ at various N . Statistical errors computed by the jackknife method are shown.

IV. DISCUSSIONS AND FUTURE PROSPECTS

The fact that $\rho_R^{(0)}(x)$ and $\langle \nu_R \rangle_0$ have the non-commutativity for the limits $\mu \rightarrow 0$ and $N \rightarrow \infty$ can

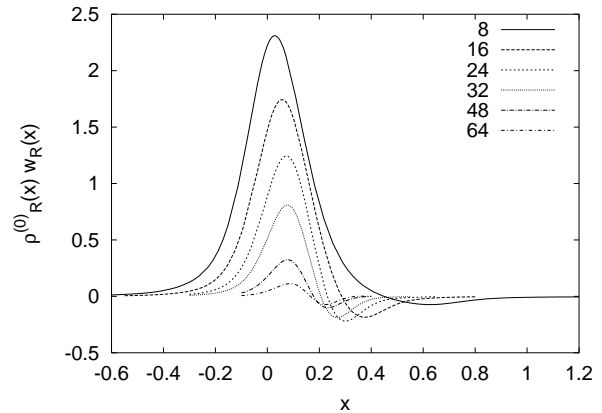


FIG. 6: The product $\rho_R^{(0)}(x) w_R(x)$, which gives the unnormalized distribution for ν_R in the full model, is plotted for $\mu = 0.2$ at various N .

be understood as a property of the phase-quenched partition function (II.11). This model undergoes a phase transition to a phase of condensed Goldstone bosons with nonzero baryon number at $\mu = m_\pi/2$ [11, 17]. For zero quark mass this phase transition takes place at $\mu = 0$. If we take the thermodynamic limit before the $\mu \rightarrow 0$ limit, the observables are calculated in a Bose-condensed phase. If the limits are taken in the opposite order, the ground state is the regular chirally broken vacuum state without Bose condensate. For this reason we obtain different values for observables depending on the order of the limits. For example, if the chiral condensate $\langle \Sigma \rangle_0$ is calculated before the $\mu \rightarrow 0$ limit, we find $\langle \Sigma \rangle_0 = 0$, whereas if we take the $\mu \rightarrow 0$ limit first, we find $\langle \Sigma \rangle_0 \neq 0$. Another example is $\frac{\partial}{\partial \mu} \langle \nu \rangle_0$, which vanishes if the $\mu \rightarrow 0$ limit is taken before the thermodynamic limit, while it is equal to unity if the limits are taken in the opposite order.

These two domains are separated by the weak non-hermiticity limit [18], where the thermodynamic limit is taken at fixed $\mu^2 N$. This is the domain where the real part of the eigenvalues is of the order of the average spacing of the eigenvalues (the eigenvalues are purely imaginary for $\mu = 0$), and quantities such as the average spectral density of the Dirac operator can be obtained analytically in this limit [19].

Mathematically, the boundary $\mu^2 N$ gives the “average” radius of convergence of the perturbative expansion of the fermion determinant in powers of μ . According to Kato’s criterion the perturbative series is convergent if the norm of the perturbative operator is less than the level spacing. Indeed the norm of $\mu \gamma_4$ is μ^2 and the average level spacing of random matrix Dirac operator (II.2) is $\sim 1/N$.

The Bose condensed phase is not present in the full partition function (II.1). Observables depend smoothly on μ for $\mu < \mu_c \neq 0$. Apparently the phase oscillations of the fermion determinant completely wipe out this phase transition. However, because reweighting methods are

based on the phase-quenched partition function, we see traces of the non-commutativity of the $\mu \rightarrow 0$ limit and the thermodynamic limit at intermediate steps of the calculation.

It is expected that such non-commutativity appears also when one studies real QCD at finite baryon density by reweighting type methods, and the transition occurs when the system size becomes larger than $V_{\text{tr}} \simeq \frac{\text{const.}}{\mu^2}$. The system size in the recent works at small μ [1, 2, 3, 4, 5] may be below the transition point, but the transition will occur if one goes to larger μ for the same system size.

Since the non-commutativity cancels in the end results for physical observables in the full model, the transition is not a physical one, but it should rather be considered as a property of the reweighting type methods. We hope that our results will be useful when one tries to go beyond the small μ regime in real QCD. It should also be mentioned that the conjectured superconducting phase may be easier to access from the other extreme, namely from the large μ regime, where the fluctuation of the phase becomes milder again according to the results in RMT [10].

Acknowledgments

We are grateful to Misha Stephanov for valuable comments. J.A. acknowledges the support by the EU network on ‘‘Discrete Random Geometry’’, grant HPRN-CT-1999-00161 as well as by *MaPhySto*, Network of Mathematical Physics and Stochastics, funded by a grant from Danish National Research Foundation. K.N.A.’s research was partially supported by RTN grants HPRN-CT-2000-00122, HPRN-CT-2000-00131 and HPRN-CT-1999-00161 and the INTAS contract N 99 0590. The work of J.N. was supported in part by Grant-in-Aid for Scientific Research (No. 14740163) from the Ministry of Education, Culture, Sports, Science and Technology. J.V. was supported in part by U.S. DOE Grant No. DE-FG-88ER40388.

V. APPENDIX

In this Appendix we briefly describe the situation with the imaginary part ν_I of the quark number density. The weight factor $w_I(x)$ becomes $w_I(x) \equiv 0$ at $\mu = 0$ for any N , and it also becomes $w_I(x) \equiv 0$ in the large N limit for any $\mu \neq 0$. However the two extreme cases are not connected smoothly. In Fig. 7 we plot the weight factor $w_I(x)$ for $\mu = 0.1$ and $\mu = 0.2$ at $N = 8, 16, 32$.

Since $w_I(x)$ is an odd function due to symmetry, it crosses the origin. A linear regime is seen to extend from the origin as μ goes to zero for fixed N . We extract the slope in the linear regime, and plot it as a function of μ in Fig. 8. At small μ , the slope can be fitted nicely by

$$\sigma_I(\mu, N) \sim -\alpha_I(N) \mu, \quad (\text{V.33})$$

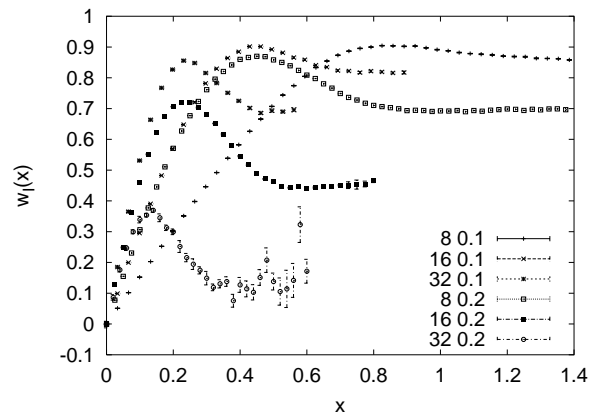


FIG. 7: The weight factor $w_I(x)$ is plotted for $\mu = 0.1$ and 0.2 at $N = 8, 16, 32$.

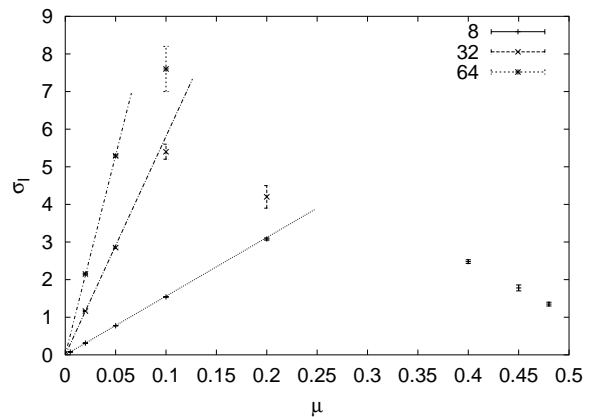


FIG. 8: The slope $\sigma_I(\mu, N)$ of the weight factor $w_I(x)$ in the linear regime is plotted against μ for $N = 8, 32, 64$. For sufficiently small μ , it fits well to $\sigma_I(\mu, N) \sim -\alpha_I(N) \mu$.

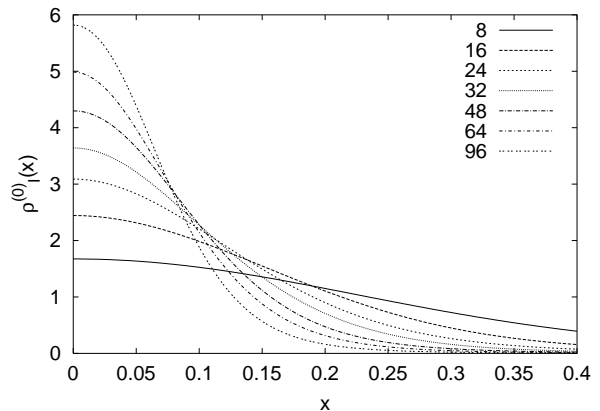


FIG. 9: The function $\rho_I^{(0)}(x)$ is plotted for $N = 8, 16, 24, 32, 48, 64, 96$ at $\mu = 0.2$.

where the coefficient $\alpha_I(N)$ grows linearly with N . Thus we find that the weight factor $w_I(x)$ has similar non-commutativity as $w_R(x)$.

On the other hand, $\rho_I^{(0)}(x)$ does not depend much on μ , and the peak at $x = 0$ grows smoothly with N as one

can see from Fig. 9. The end result for $i\langle\nu_I\rangle$ does not have the non-commutativity (See Table I), but the cancellation in this case occurs between the numerator and the denominator of (II.17), which makes it less obvious than the situation with $\langle\nu_R\rangle$.

-
- [1] Z. Fodor and S. D. Katz, *Phys. Lett. B* **534**, 87 (2002).
 - [2] Z. Fodor and S. D. Katz, *JHEP* **0203**, 014 (2002).
 - [3] C. R. Allton *et al.*, *Phys. Rev.* **D66**, 074507 (2002).
 - [4] P. de Forcrand and O. Philipsen, *Nucl. Phys.* **B642**, 290 (2002).
 - [5] M. D'Elia and M. P. Lombardo, *Phys. Rev.* **D67**, 014505 (2003).
 - [6] S. Ejiri, [hep-lat/0401012](#).
 - [7] K. N. Anagnostopoulos and J. Nishimura, *Phys. Rev. D* **66**, 106008 (2002).
 - [8] V. Azcoiti, G. Di Carlo, A. Galante and V. Laliena, *Phys. Rev. Lett.* **89**, 141601 (2002).
 - [9] S. Muroya, A. Nakamura, C. Nonaka and T. Takaishi, *Prog. Theor. Phys.* **110**, 615 (2003).
 - [10] J. Ambjørn, K. N. Anagnostopoulos, J. Nishimura and J. J. Verbaarschot, *J. High Energy Phys.* **10**, 062 (2002).
 - [11] M. A. Stephanov, *Phys. Rev. Lett.* **76**, 4472 (1996).
 - [12] J. J. Verbaarschot and T. Wettig, *Ann. Rev. Nucl. Part. Sci.* **50**, 343 (2000).
 - [13] M. A. Halasz, A. D. Jackson and J. J. Verbaarschot, *Phys. Rev. D* **56**, 5140 (1997).
 - [14] M. A. Halasz, J. C. Osborn, M. A. Stephanov and J. J. Verbaarschot, *Phys. Rev. D* **61**, 076005 (2000).
 - [15] J. Ambjørn, K. N. Anagnostopoulos, J. Nishimura and J. J. Verbaarschot, [hep-lat/0310004](#).
 - [16] J. Nishimura, [hep-lat/0310018](#).
 - [17] A. Gocksch, *Phys. Rev. D* **37**, 1014 (1988).
 - [18] Y. V. Fyodorov, B. A. Khoruzhenko and H. J. Sommers, *Phys. Lett. A* **226**, 46 (1997).
 - [19] K. Splittorff and J. J. M. Verbaarschot, [hep-th/0310271](#).
 - [20] We take this opportunity to correct the proceedings [16], where it was wrongly stated that the free energy *has* a discontinuity.